

Continuous-variable quantum authentication of physical unclonable keys: Security against an emulation attack

Georgios M. Nikolopoulos^{1,*}

¹*Institute of Electronic Structure & Laser, FORTH, P.O. Box 1385, GR-70013 Heraklion, Greece*
(Dated: September 19, 2018)

We consider a recently proposed entity authentication protocol, in which a physical unclonable key is interrogated by random coherent states of light, and the quadratures of the scattered light are analysed by means of a coarse-grained homodyne detection. We derive a sufficient condition for the protocol to be secure against an emulation attack, in which an adversary knows the challenge-response properties of the key, and moreover he can access the challenges during the verification. The security analysis relies on Holevo's bound and Fano's inequality, and suggests that the protocol is secure against the emulation attack for a broad range of physical parameters that are within reach of today's technology.

PACS numbers: 03.67.Dd, 42.50.-p

I. INTRODUCTION

The development of entity authentication (identification) protocols (EAPs), which are robust against cloning and other impersonation strategies, is an outstanding task in modern cryptography [1, 2]. Currently, optical physical unclonable keys (PUKs) are considered to be the most promising candidates for the development of highly robust EAPs [3–11]. Typically, optical PUKs are materialized by multiple-scattering optical media, where disorder is introduced during fabrication. Hence, faithful cloning of an optical PUK requires the exact positioning (on a nanometer scale) of millions of scatterers with the exact size and shape, which is considered to be a formidable challenge not only for current, but for future technologies as well [5, 6, 9].

Optical PUK-based authentication protocols [3–11] rely on two-stage challenge-response mechanisms, analogous to the ones used in everyday transactions with smart cards (e.g., credit cards), at automatic teller machines, and point of sale terminals [1, 2]. The *enrolment stage* is performed only once by the manufacturer (or the authority that issues and distributes the PUKs), well before the PUK is given to a user. It aims at the faithful characterization of the PUK with respect to its optical responses to a finite set of random challenges, that is to light pulses (probes) with random parameters. The set of challenge-response pairs (CRPs) is stored at a server, and the PUK is given to a user, together with a personal identification number (PIN), which is also saved at the same server. The *verification stage* takes place each time the holder of the PUK has to be authenticated to the system, it is performed by a legitimate verifier, who is connected to the server over a secure and authenticated classical channel, and involves two steps. First, the user inserts his PUK in a verification device and types in his secret PIN. In this way the user is verified to the PUK, thereby preventing

someone who has stolen the PUK and does not know the PIN, to pass himself as the user. The PIN is sent to the server over the classical channel, and if it is valid the verifier has to decide whether the PUK is authentic or not. To this end, the server sends to the verifier (over the classical channel), a moderate number of challenges, chosen at random from the recorded challenges in the database. The verifier interrogates sequentially the PUK with each one of the challenges, and the corresponding responses are sent back to the server, where they are compared to those in the database. The server decides upon the acceptance (rejection) of the PUK, based on some algorithm that takes into account the deviations from the expected responses. The number of challenges that are used in the verification stage depends on the EAP under consideration, but in any case it should be such that the verification stage takes place within a reasonable amount of time, say few seconds (see also related discussion in Sec. II B).

Most of the proposed optical EAPs that rely on PUKs, exploit the speckle of the scattered light and pertain to classical challenges [3–8]. If the verification set-up is not tamper-resistant, such EAPs are vulnerable to emulation attacks, in which the adversary has stolen the PIN and knows the challenge-response properties of the PUK. Hence, his task is to intercept each challenge during the verification stage, measure it, and send to the verifier the expected response [9]. This is a highly realistic scenario [12], and if the adversary can access the classical challenges during the verification, nothing prevents him from determining them completely, without introducing any errors.

The robustness of PUK-based optical EAPs against emulation attacks can be increased considerably if the PUK is challenged by quantum states of light. When the quantum state is chosen at random from a set of non-orthogonal states, the laws of quantum physics prevent an adversary to discriminate unambiguously between different states, while information gain can be obtained at the cost of disturbing the state of the probe [13]. Hence,

* nikolg@iesl.forth.gr

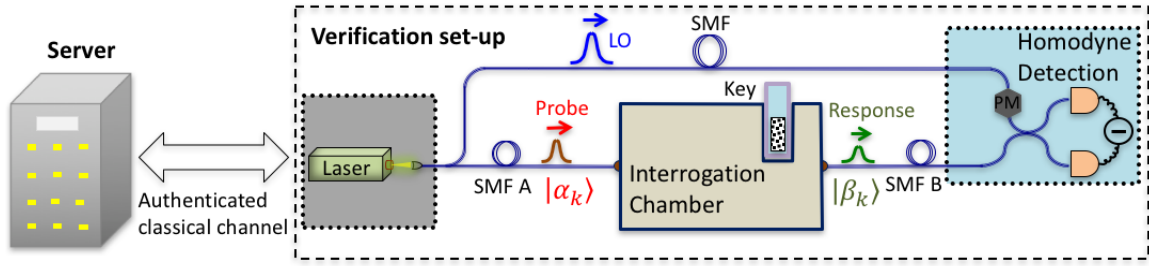


FIG. 1. (Color online) A schematic representation of the PUK-based optical EAP under consideration.

if the EAP is designed judiciously so that the response of the PUK depends on the quantum state of the probe, then it is highly unlikely for an adversary to estimate correctly all of the challenges used during the verification of a PUK without introducing any errors. In this spirit, Goorden *et al* have proposed and implemented an authentication protocol, in which the challenges pertain to attenuated laser pulses with shaped wavefronts [9]. The mean number of photons per mode in the challenge is less than 1, which prevents an adversary from characterizing fully the wavefront of the challenge.

Recently, we proposed an alternative PUK-based optical EAP, which relies on standard wavefront-shaping and homodyne-detection techniques [11]. In the framework of a tamper-resistant verification set-up, it was shown that the protocol offers collision resistance, and it is robust against PUK cloning. The present work focuses on the verification stage of the protocol, and in particular on the authentication of the PUK to the system. Our main task is to investigate the robustness of the protocol against an emulation attack, in which a cheater has obtained access to the database without being noticed [12], and moreover he has been able to bypass the actual verification set-up, thereby directing each probe to his detection device for analysis.

II. AUTHENTICATION SCHEME

The verification set-up has been discussed in detail elsewhere [11], and for the sake of completeness, its main components are outlined in Fig. 1. It consists of three major parts namely, the laser source, the interrogation chamber, and the homodyne-detection chamber. Light from the laser source is split into two parts: a weak probe that is directed to the interrogation chamber by means of a single-mode fiber (SMF), and a strong local oscillator (LO), which serves as a reference in the homodyne detection (HD). The interrogation chamber is basically a standard wavefront-shaping set-up, in which the light from SMF A is collimated, and its spatial phase pattern is modulated by means of a phase-only spatial light-modulator (SLM) [14–23]. The shaped wavefront is then focused on the PUK, and the phase mask of the SLM is optimized so that the multiple-scattered light is mainly

directed to a prescribed transversal spatial mode of the output plane (target mode), where it is coupled to SMF B [14–23]. The collected scattered light is transferred to the HD set-up, where its quadratures are analysed.

Standard wavefront shaping set-ups allow for the control of hundreds and even thousands of spatial modes, and the intensity of the scattered light is enhanced relative to the unoptimized case by a factor $\mathcal{E} \gg 1$. Due to noise and imperfections, the enhancement factor that can be achieved in practise is below the ideally expected value of $\pi\mathcal{N}/4 \simeq 0.78\mathcal{N}$ [15, 20, 24, 25], where \mathcal{N} is the number of modes that can be controlled in the wavefront-shaping set-up. The reported ratios \mathcal{E}/\mathcal{N} in related experiments range from about 0.2 to about 0.6 [24].

A. Challenge-response pairs

The enrolment of a PUK takes place only once, and aims at the generation of a finite set of CRPs, which is stored in a server, and will be used for the authentication of the PUK. The enrolment is performed by the manufacturer well before the PUK is given to a user, and we naturally assume that the enroller has all the time and the resources needed so that the accuracy in the estimation of the response of the PUK to each one of the challenges, is considerably higher than the accuracy in the verification stage [11]. Throughout this work we consider identical set-ups for the enrolment and the verification stages, which operate in the diffusive limit [26, 31], and all of their specifications (i.e., transmission losses, imperfections, etc) are publicly known.

Our scheme accepts various types of challenges, pertaining to the probe state, the target mode and the phase mask of the SLM. In this work, we consider a rather simple challenge, by assuming that the target mode (i.e., the position of SMF B at the output plane) is fixed and publicly known. Hence, a challenge has two parts and it is of the form

$$C_k = \{k, \Phi(\mathcal{K}) : k \in \mathbb{Z}_N\}, \quad (1)$$

with the integer k chosen at random from a uniform distribution over $\mathbb{Z}_N \equiv \{0, 1, 2, \dots, N-1\}$, while the integer $N \gg 1$ is a publicly known constant. We consider coherent probe states with the same, publicly known mean

number of photons μ_P , and random phase φ_k i.e.,

$$|\alpha_k\rangle := |\sqrt{\mu_P}e^{i\varphi_k}\rangle, \text{ with } \varphi_k := \frac{2\pi k}{N}. \quad (2)$$

Hence, the integer k identifies uniquely the probe state. Finally, Φ denotes the optimal phase-mask for the SLM, which maximizes the intensity of the scattered light in SMF B, and depends on the scattering matrix of the PUK \mathcal{K} , as well as various parameters of the fixed set-up, which are assumed to be publicly known and are not shown in Eq. (1). It is worth emphasizing here that for the optimization process used in our simulations [11], the optimal phase mask of the SLM does not depend on the phase of the probe [27]. In fact, it has been demonstrated both theoretically and experimentally that an optimal phase mask works equally well, regardless the quantum state of the incoming light [21–23].

The response of the PUK to a given challenge C_k , pertains to the electric field $\hat{E}_k(\mathcal{K}) := \hat{X}_k(\mathcal{K}) + i\hat{Y}_k(\mathcal{K})$ in SMF B (see table I). For later convenience, let us introduce here the generalized θ -quadrature $\hat{Q}_k(\theta)$ of the field in SMF B, with $\hat{Q}_k(0) = \hat{X}_k$ and $\hat{Q}_k(\pi/2) = \hat{Y}_k$. It has been shown that in the diffusive limit, the field in SMF B is also in a coherent state, say $|\beta_k\rangle$, with the expectation value of θ -quadrature given by (see also appendix A) [11]

$$\langle \hat{Q}_k(\theta) \rangle := \sqrt{2\mu_R} \cos(\psi_k - \theta), \quad (3a)$$

with

$$\mu_R = \mathcal{E}|\mathcal{F}|^2\mu_P, \quad (3b)$$

$$\psi_k := \arg(\mathcal{F}) + \varphi_k. \quad (3c)$$

The factor \mathcal{F} is a complex number that depends on the PUK \mathcal{K} , the phase-mask of the SLM and various other publicly-known parameters of the set-up, while $|\mathcal{F}|^2 < 1/N$ [11]. As mentioned above, the enhancement factor \mathcal{E} depends on the details of set-up, and in practise it does not exceed the ideal value of $\pi N/4$. Hence, we expect $\mu_R < \pi\mu_P/4 \approx 0.78\mu_P$. For a fixed verification set-up and a given PUK, $\arg(\mathcal{F})$ is a global phase, which shifts the phase of the probe φ_k , and thus it is not expected to affect the following security analysis (see related discussion in Sec. III C). In the attack to be considered below, the adversary is assumed to know the CRPs for the PUK [12], while \mathcal{F} is publicly known.

For a fixed set-up and given PUK, a CRP is uniquely identified by the choice of the probe i.e., by the choice of the integer $k \in \mathbb{Z}_N$, because throughout this work, all of the parameters of the set-up, including μ_P and the position of SMF B, are assumed to be publicly known. As will be explained below, even if an adversary has obtained access to the server where the database of CRPs is stored, the response of the PUK to a randomly chosen probe state $|\alpha_k\rangle$ cannot be estimated without knowledge of the integer k .

To suppress notation, the dependence of Φ and \hat{E}_k on the PUK \mathcal{K} , is not explicitly shown in the following

TABLE I. Illustration of a set of CRPs used for authentication of a PUK. The angles $\theta = 0$ and $\pi/2$ refer to the quadratures \hat{X}_k and \hat{Y}_k of the response field \hat{E}_k , respectively.

PIN			
Challenge		Response	
k	Phase mask	$\theta = 0$	$\theta = \pi/2$
0	Φ	$\langle \hat{X}_0 \rangle$	$\langle \hat{Y}_0 \rangle$
1		$\langle \hat{X}_1 \rangle$	$\langle \hat{Y}_1 \rangle$
2		$\langle \hat{X}_2 \rangle$	$\langle \hat{Y}_2 \rangle$
\vdots		\vdots	\vdots
$N-1$		$\langle \hat{X}_{N-1} \rangle$	$\langle \hat{Y}_{N-1} \rangle$

sections. In the emulation attack under consideration the attacker bypasses the interrogation chamber, and thus the PUK does not enter the related security analysis. Before we proceed with the attack, however, it will be helpful to discuss briefly the verification of a PUK, in the ideal scenario of tamper-resistant verification set-up and secure server.

B. Verification in the absence of cheating

By contrast to the enrolment stage, verification takes place each time a PUK has to be authenticated by a legitimate verifier, who has access to the server (where the database of CRPs is located) over a secure and authenticated classical channel. The first action of the verifier is to send the user's PIN to the server, over the classical channel. If the PIN is not valid the verification is aborted. Otherwise, the server returns a number of challenges, say $\{C_1, C_2, \dots, C_M\}$ [see Eq. (1)], chosen at random and independently from the registered finite set of CRPs for the PUK to be authenticated. In addition, the server sends to the verifier a sequence of random and independently chosen angles $\{\theta_1, \theta_2, \dots, \theta_M\}$, with θ_j uniformly distributed over $\{0, \pi/2\}$ [28, 29].

The verifier queries the PUK with each one of the M challenges sequentially, and records the corresponding responses. Given that the challenges are chosen at random and independently, it is sufficient to consider one of the challenges, say the j th one. The phase mask of the SLM is set to Φ , and the phase of the probe is set to $\varphi_{k_j} = 2\pi k_j/N$. The verifier measures the quadrature amplitude of the electric field of the scattered light in SMF B, by means of HD where the LO serves as the required reference [32]. More precisely, for the j th query, the LO phase is set to $\theta_j \in \{0, \pi/2\}$, and the verifier measures the quadrature $\hat{Q}_{k_j}(\theta_j)$. Assuming that the LO field is much stronger than the total scattered field, the outcome of such a measurement is a real random number q_j which, to a good accuracy, follows a normal (Gaussian) distribution $\mathcal{N}(\bar{q}_{k_j}(\theta_j), \sigma^2)$, with standard deviation $\sigma \simeq 1/\sqrt{2\eta}$, where $\eta \leq 1$ is the detection efficiency [33]. In other words, the measurement of the quadrature

$\hat{Q}_{k_j}(\theta_j)$ is equivalent to sampling from the Gaussian distribution $\mathcal{N}(\bar{q}_{k_j}(\theta_j), \sigma^2)$. The mean $\bar{q}_{k_j}(\theta_j)$ also depends on the scattering matrix of the PUK, but for the reasons discussed above, this dependence is not explicitly shown. The sequence of random outcomes $\{q_1, q_2, \dots, q_M\}$, are sent to the server over the secure and authenticated classical channel.

Aiming at practical verification tests, and in order to circumvent difficulties arising from statistical deviations in finite sampling, we proposed a verification process that employs two-bin coarse-graining of the outcomes from the M independent HDs. More precisely, in the j th sample with challenge C_j and measured quadrature $\hat{Q}_{k_j}(\theta_j)$, the server checks if the outcome q_j falls in the interval (bin)

$$\mathbb{B}_{k_j}(\theta_j) = \left[\langle \hat{Q}_{k_j}(\theta_j) \rangle - \frac{\Delta}{2}, \langle \hat{Q}_{k_j}(\theta_j) \rangle + \frac{\Delta}{2} \right], \quad (4)$$

which is centred at the expected response recorded in the database of CRPs, and has size $2\sigma \lesssim \Delta < 4\sigma$.

In the ideal scenario, where the true PUK is authenticated in a tamper-resistant verification set-up and no cheating takes place, the verifier samples from a Gaussian distribution centred at $\bar{q}_{k_j}(\theta) = \langle \hat{Q}_{k_j}(\theta_j) \rangle$, which coincides with center of the bin $\mathbb{B}_{k_j}(\theta_j)$. Hence, the probability for the outcome q_{k_j} to fall in the bin, given that the PUK is interrogated by challenge C_j and the θ_j -quadrature is measured, is given by (see appendix B)

$$P^{(0)}(\text{in}|k_j, \theta_j) = \text{Erf} \left(\frac{\bar{\Delta}}{2\sqrt{2}} \right). \quad (5)$$

The key point is that this probability is independent of k_j and θ_j , and depends only on the ratio $\bar{\Delta} := \Delta/\sigma$.

Counting the total number of queries (samples) M_{in} that resulted in an outcome within the expected bin, irrespective of the chosen challenge or the measured quadrature, the server obtains the relative frequency $f_{\text{in}} := M_{\text{in}}/M$, which is an estimate of the average probability

$$\begin{aligned} P_{\text{in}}^{(0)} &:= \sum_{k=0}^{N-1} \sum_{\theta \in \{0, \pi/2\}} p(k)p(\theta)P^{(0)}(\text{in}|k, \theta) \\ &= \frac{1}{2N} \sum_{k=0}^{N-1} \sum_{\theta \in \{0, \pi/2\}} P^{(0)}(\text{in}|k, \theta). \end{aligned} \quad (6)$$

Here, we have taken into account that k and θ are chosen at random and independently from uniform distributions over \mathbb{Z}_N and $\{0, \pi/2\}$, respectively. Substituting Eq. (5) in Eq. (6), one readily obtains

$$P_{\text{in}}^{(0)} = \text{Erf} \left(\frac{\bar{\Delta}}{2\sqrt{2}} \right). \quad (7)$$

The acceptance or rejection of the PUK is decided upon the deviation of the estimated probability f_{in} from the theoretically expected one, which in the absence of

any cheating is given by $P_{\text{in}}^{(0)}$. It has been shown that a sample of size at least as large as

$$M_{\text{th}} := \frac{3 \ln(2\zeta^{-1})}{\varepsilon^2}, \quad (8)$$

suffices for the estimate f_{in} to satisfy

$$\Pr(|f_{\text{in}} - P_{\text{in}}^{(0)}| \geq \varepsilon) < \zeta, \quad (9)$$

where $\zeta \ll 1$ is the uncertainty, and $\varepsilon \ll P_{\text{in}}^{(0)}$ is the absolute error [11]. For $M > M_{\text{th}}$ one can be $100(1 - \zeta)\%$ confident that in the absence of any cheating, the estimate will lie within an interval of size 2ε around the theoretically expected probability i.e., $|f_{\text{in}} - P_{\text{in}}^{(0)}| < \varepsilon$. So, a PUK is accepted if $|f_{\text{in}} - P_{\text{in}}^{(0)}| < \varepsilon$, and is rejected otherwise.

According to Eq. (8), samples of size $M \simeq 2.3 \times 10^7$ suffice for verification tests of error $\varepsilon \simeq 10^{-3}$ and confidence 99.9%. Assuming that the separation distances between the different components of the verification set-up are of the order of meters or tens meters, and for HD bandwidth $\sim 10 - 100$ MHz (depending on the implementation), the total verification time is expected to be a few seconds [11].

The interested reader may refer to Ref. [11], for a detailed discussion on the different stages of the protocol, a full description of its implementation, as well as for a thorough analysis on its security in the case of tamper-resistant verification set-up and secure server. Both of these assumptions are relaxed in the emulation attack discussed in the following section. In this case, the cheater's intervention is expected to introduce errors in the responses of the PUK to the various challenges, thereby enforcing the verifier to sample from photocount distributions, which are shifted relative to the expected bins. The protocol is secure only if the aforementioned coarse-grained HD can detect these shifts, which is not true for any combination of μ_P and N . For the sake of convenience, the main parameters entering the following security analysis are summarized in table II.

III. EMULATION ATTACK AND SECURITY

Consider the cheating strategy of Fig. 2, in which the adversary aims at the impersonation of the legitimate user, without having the true PUK. The adversary does not have access either to the laser source or to the HD set-up of the verifier, but he has hacked the server, and has obtained the PIN of the user he intends to impersonate, together with a copy of the CRPs of his PUK [12]. Moreover, he has installed his own perfect line, thereby bypassing the verification set-up, and directing each probe to his lab. Clearly, there is no need for the adversary to have the user's PUK, because he has a copy of the corresponding list of CRPs [34]. If the cheater can estimate reliably the probe state, he can prepare the right response by looking up the set of all possible CRPs,

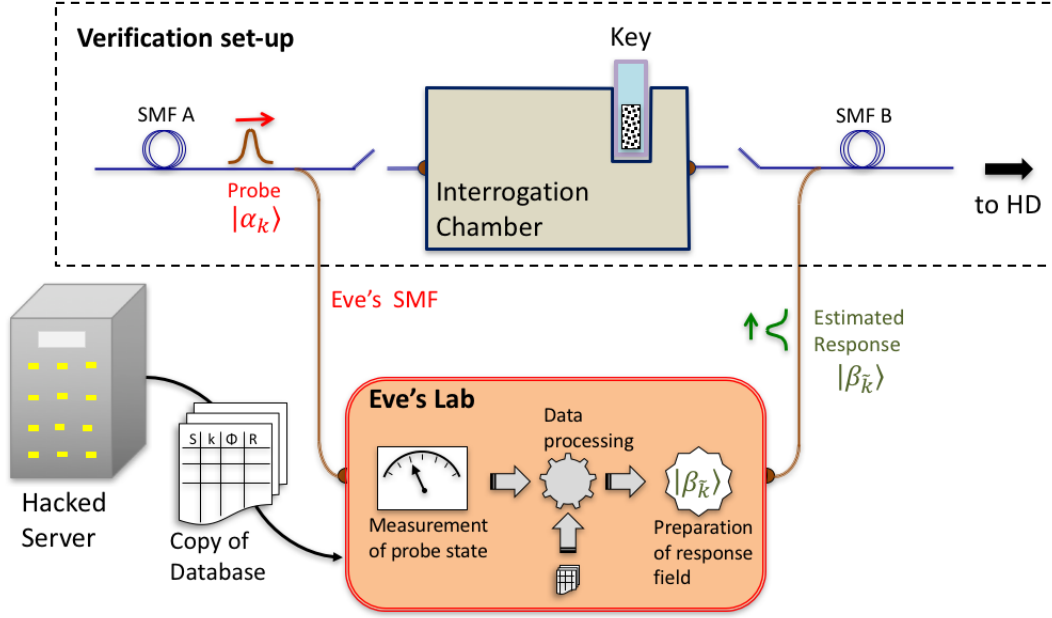


FIG. 2. (Color online) A schematic representation of the emulation attack considered throughout this work. An adversary who knows the set of all possible CRPs pertinent to a PUK, but he does not possess the actual PUK, bypasses the interrogation chamber, thereby directing each probe in his ideal lab [34]. The probe is measured, and a response state, which is consistent with the outcome of the measurement and the list of possible CRPs, is sent to the HD set-up of the verifier (not shown here).

TABLE II. List of the main parameters in the present security analysis. The PIN as well as the scattering matrix of the PUK and/or the challenge-response pairs are assumed to have leaked to the adversary (see Sec. I and remark [12]).

Parameter	Symbol	Property
Mean number of photons in probe	μ_P	Public
Phase of probe	φ_k	Private
Total number of phases	N	Public
Mean number of photons in response	μ_R	Public
PIN	-	Leaked
Position of SMF B	-	Public
PUK	\mathcal{K}	Private
Scattering matrix of PUK	-	Leaked
Number of controlled modes	\mathcal{N}	Public
Phase mask of SLM	Φ	Leaked
Enhancement factor	\mathcal{E}	Public
Detection efficiency	η	Public
-	\mathcal{F}	Public
Other specifications of set-up	-	Public
Bin size	Δ	Public
Error in verification tests	ε	Public
Confidence in verification tests	ζ	Public
Challenge-response pairs	CRPs	Leaked

and send to the HD set-up of the verifier a quantum state that is consistent with the expected response of the true PUK. This is possible for classical challenges, because nothing prevents the cheater from estimating precisely all of the characteristics of the probe, without introducing any errors. Hence, any EAP where the PUK is chal-

lenged by classical signals [4–8] is susceptible to such an emulation attack. The situation is fundamentally different in our protocol, because the PUK is interrogated by random non-orthogonal quantum states. According to quantum mechanics, non-orthogonal quantum states cannot be reliably distinguished [13], and thus the adversary’s intervention is expected to introduce errors in the coarse-grained HD.

A. Error probability

In our scheme, the probe state is a pure coherent state $|\alpha_k\rangle$, with random phase. From the adversary’s point of view, before any measurements, the probe’s state is a mixture of the form

$$\rho = \frac{1}{N} \sum_{k=0}^N |\alpha_k\rangle\langle\alpha_k|. \quad (10)$$

The average information that an adversary can extract from the state (10) is limited by the Holevo bound χ , which is given by the von Neumann entropy $S(\rho) \equiv -\text{Tr}[\rho \log_2(\rho)]$ i.e.,

$$\chi = S(\rho). \quad (11)$$

For given μ_P and N , the entropy $S(\rho)$ can be calculated numerically. A simple analytic expression can be obtained in the continuous limit $N \rightarrow \infty$, where $S(\rho)$ approximates the entropy of the Poisson distribution, which

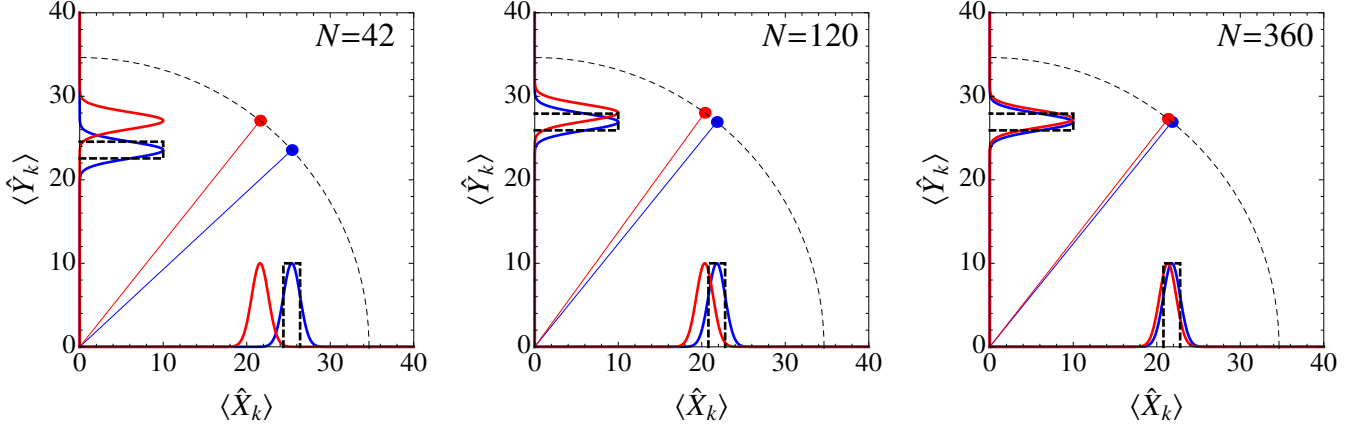


FIG. 3. (Color online) Two neighbouring coherent states in phase-space representation (blue and red disks), with the same mean number of photons $\mu = 600$, and phases that differ by $2\pi/N$, for three different values of N . The radius of the disks is equal to the shot noise i.e., $1/\sqrt{2}$. The Gaussians show the corresponding photocount distributions for each quadrature, and their standard deviation is $\sigma = 1/\sqrt{2\eta}$, for $\eta = 0.5$. The dashed box represents an interval of size $\Delta = 2\sigma$.

for $\mu_P \gtrsim 10$ is given by

$$\mathcal{H}_\infty(\mu_P) \simeq \log_2(\sqrt{2\pi e \mu_P}). \quad (12)$$

The overlap of neighbouring probe states is determined by the number of different phases N , and the mean number of photons μ_P . The larger N becomes for a given μ_P , the larger the overlap becomes (see Fig. 3).

Our scheme involves $M \gg 1$ equivalent samples (queries), and for each one of them the positive integer k is chosen at random and independently from \mathbb{Z}_N . In the emulation attack under consideration, the adversary has a copy of all the relevant CRPs. Hence, for each one of the samples, he intercepts the probe state and measures it, so that to obtain an estimate of the integer k , say \tilde{k} . By looking up the set of CRPs, he finds the expected response $\{\langle \hat{X}_{\tilde{k}} \rangle, \langle \hat{Y}_{\tilde{k}} \rangle\}$ that corresponds to \tilde{k} . Subsequently, he prepares and sends to the HD (through SMF B) the coherent state $|\beta_{\tilde{k}}\rangle$ which satisfies $\langle \beta_{\tilde{k}} | \hat{E} | \beta_{\tilde{k}} \rangle = \langle \hat{X}_{\tilde{k}} \rangle + i \langle \hat{Y}_{\tilde{k}} \rangle$.

It may happen that in a single sample the adversary will obtain the right value of k . In this case, the centres of the Gaussian photocount distributions for the two quadratures coincide with the centres of the corresponding bins i.e., $\langle \hat{X}_{\tilde{k}} \rangle = \langle \hat{X}_k \rangle$ and $\langle \hat{Y}_{\tilde{k}} \rangle = \langle \hat{Y}_k \rangle$. However, if μ_P and N are such that there is significant overlap between different possible probe states, it is impossible for the adversary to distinguish them reliably, and thus to obtain the right value of k in all of the M queries. In other words, it is inevitable for the adversary to make wrong guesses about the state of the probe in some queries, and thus send to the HD set-up a response state $|\beta_{\tilde{k}}\rangle$ for which the centres of the photocount distributions are shifted relative to the expected bins i.e., $\langle \hat{X}_{\tilde{k}} \rangle \neq \langle \hat{X}_k \rangle$ and $\langle \hat{Y}_{\tilde{k}} \rangle \neq \langle \hat{Y}_k \rangle$. In these cases, the probability for the outcome of the HD to fall in the bin is smaller than the probability of Eq. (5).

It is sufficient for our purposes to consider the probability p_{err} for the adversary to infer a wrong value of k , based on the outcome of his measurement on probe state $|\alpha_k\rangle$, and perhaps some additional post processing. According to Fano's inequality, when k is uniformly distributed on \mathbb{Z}_N the probability of error satisfies [13]

$$\mathcal{H}(p_{\text{err}}) + p_{\text{err}} \log_2(N-1) \geq \log_2(N) - \chi, \quad (13)$$

with the Holevo bound given by Eq. (11). Solving this inequality for a given state ρ , one obtains a lower bound on the error probability, say $p_{\text{err}}^{(\text{low})}$.

B. Security condition

As discussed in Sec. II B, in the EAP under consideration acceptance or rejection of a PUK is decided upon the estimated average probability for an outcome to fall in a bin. Given that the cheater's intervention will inevitably introduce errors, we need to find how these errors affect the estimated probability in the verification stage.

Consider a single query, where the verifier sends $|\alpha_k\rangle$, the cheater infers \tilde{k} and sends the coherent state $|\beta_{\tilde{k}}\rangle$ to the HD set-up of the verifier. As discussed above, the wrong guess of the cheater will enforce the verifier to sample from a Gaussian photocount distribution that is shifted relative to the expected bin. More precisely, the conditional probability for the outcome of the HD to fall in the expected bin $\mathbb{B}_k(\theta)$, given that the verifier has chosen k , the adversary has inferred \tilde{k} , and the verifier measures the θ quadrature of the field is given by (see

appendix B)

$$P(\text{in}|k, \tilde{k}, \theta) = \frac{1}{2} \left\{ \text{Erf} \left[\frac{2S(k, \tilde{k}, \theta) + \Delta}{2\sqrt{2}\sigma} \right] - \text{Erf} \left[\frac{2S(k, \tilde{k}, \theta) - \Delta}{2\sqrt{2}\sigma} \right] \right\}, \quad (14)$$

where

$$S(k, \tilde{k}, \theta) := \langle \hat{Q}_{\tilde{k}}(\theta) \rangle - \langle \hat{Q}_k(\theta) \rangle, \quad (15)$$

and $\langle \hat{Q}_{\tilde{k}}(\theta) \rangle$ is also given by Eq. (3), for index \tilde{k} instead of k . Recall here that $\langle \hat{Q}_k(\theta) \rangle$ is the centre of the bin when the probe state $|\alpha_k\rangle$ has been used and the θ -quadrature is measured (see Eq. 4). When the adversary infers the correct value of k i.e., for $\tilde{k} = k$, then $\langle \hat{Q}_{\tilde{k}}(\theta) \rangle$ coincides with the mean of the Gaussian photocount distribution the verifier samples from. When the adversary fails to infer the correct value of k , i.e., for $\tilde{k} \neq k$, the photocount distribution is centred at $\hat{Q}_{\tilde{k}}(\theta)$. Hence, $S(k, \tilde{k}, \theta)$ is the shift of the photocount distribution relative to the bin, which is zero only in the case of $\tilde{k} = k$, and non-zero otherwise. In the former case, Eq. (14) reduces to Eq. (5), which shows that the cheater's intervention has not affected the photocount statistics expected by the server in the absence of cheating.

Given that the server asks the verifier to sample from both quadratures at random and independently, after M queries the verifier will obtain an estimate of the average

probability

$$P_{\text{in}} = \sum_{k=0}^{N-1} \sum_{\tilde{k}=0}^{N-1} \sum_{\theta} P(\text{in}, k, \tilde{k}, \theta). \quad (16)$$

The arguments of Sec. II B are also valid in the case of cheating. That is, as long as $M > M_{\text{th}}$ and $\varepsilon \ll P_{\text{in}}$, with high probability the estimate of the server will lie within an interval of size 2ε around the theoretically expected probability, which in the presence of cheating is P_{in} instead of $P_{\text{in}}^{(0)}$ i.e., we have

$$|f_{\text{in}} - P_{\text{in}}| < \varepsilon, \quad (17)$$

with high probability.

The probability P_{in} is different from the corresponding probability in the absence of cheating $P_{\text{in}}^{(0)}$, and can be bounded from above as follows (see appendix C)

$$P_{\text{in}} \leq (1 - p_{\text{err}})P_{\text{in}}^{(0)} + p_{\text{err}} \max_{k, \tilde{k}} \{P(\text{in}|k, \tilde{k})\}_{k \neq \tilde{k}}, \quad (18)$$

where $P_{\text{in}}^{(0)}$ is given by Eq. (7) and

$$P(\text{in}|k, \tilde{k}) := \sum_{\theta \in \{0, \pi/2\}} p(\theta) P(\text{in}|k, \tilde{k}, \theta).$$

Recalling that both quadratures are equally probable, and using Eqs. (14), (15) we have

$$P(\text{in}|k, \tilde{k}) = \frac{1}{4} \sum_{\theta \in \{0, \pi/2\}} \left\{ \text{Erf} \left[\frac{2(\langle \hat{Q}_{\tilde{k}}(\theta) \rangle - \langle \hat{Q}_k(\theta) \rangle) + \Delta}{2\sqrt{2}\sigma} \right] - \text{Erf} \left[\frac{2(\langle \hat{Q}_{\tilde{k}}(\theta) \rangle - \langle \hat{Q}_k(\theta) \rangle) - \Delta}{2\sqrt{2}\sigma} \right] \right\}. \quad (19)$$

where $\langle \hat{Q}_{\tilde{k}}(\theta) \rangle$ and $\langle \hat{Q}_k(\theta) \rangle$ are given by Eq. (3) for \tilde{k} and k , respectively. Moreover, using Eqs. (7) and (14), one can readily confirm that $\max_{k, \tilde{k}} \{P(\text{in}|k, \tilde{k})\}_{k \neq \tilde{k}} \leq P_{\text{in}}^{(0)}$, and thus

$$P_{\text{in}}^{(0)} - P_{\text{in}} \geq p_{\text{err}} \left(P_{\text{in}}^{(0)} - \max_{k, \tilde{k}} \{P(\text{in}|k, \tilde{k})\}_{k \neq \tilde{k}} \right) \geq 0, \quad (20)$$

where equality holds only in the absence of cheating.

As described in Sec. II B, a PUK is accepted only if the estimate f_{in} lies within an interval of size $2\varepsilon \ll 1$ around $P_{\text{in}}^{(0)}$, and not around P_{in} . So, the cheating will be detected if

$$P_{\text{in}}^{(0)} - P_{\text{in}} > 2\varepsilon. \quad (21)$$

Indeed, in view of inequality (17), inequality (21) implies $P_{\text{in}}^{(0)} - f_{\text{in}} > \varepsilon$, with high probability. That is, the detected deviations from $P_{\text{in}}^{(0)}$ exceed the statistical devi-

ations, and can be attributed only to some sort of cheating. Of course, one cannot infer the precise type of the cheating, but this is not of importance for the security of the protocol.

From inequalities (20) and (21), we obtain that the condition

$$p_{\text{err}}^{(\text{low})} \left(P_{\text{in}}^{(0)} - \max_{k, \tilde{k}} \{P(\text{in}|k, \tilde{k})\}_{k \neq \tilde{k}} \right) > 2\varepsilon, \quad (22)$$

suffices to ensure the security of the protocol, where $p_{\text{err}}^{(\text{low})}$ is a lower bound on the error probability p_{err} obtained through inequality (13).

Condition (22) is the main result of this work. The left-hand side (l.h.s) of the inequality is a function of μ_P , N , μ_R , η , $\bar{\Delta}$, and for later convenience it will be denoted by D . For a fixed verification set-up, with known parameters, condition (22) allows one to estimate combinations of μ_P , N and ε , so that the protocol is secure against the emulation attack under consideration, in the sense that

the cheating will be detected, and the adversary will fail to pass himself as the legitimate user.

C. Numerical results

We performed simulations for various combinations of the parameters that enter inequality (22). More precisely, for a given pair of $\{\mu_P, N\}$, we calculated the entropy of the density matrix (10), which is equal to the Holevo bound (11). The estimated bound was used in inequality (13) to obtain the lower bound $p_{\text{err}}^{(\text{low})}$ on the error probability. The difference of probabilities in inequality (22) was estimated numerically through Eqs. (7), (19), and (3), for various combinations of μ_R , $\bar{\Delta}$ and η .

The difference $\langle \hat{Q}_{\tilde{k}}(\theta) \rangle - \langle \hat{Q}_k(\theta) \rangle$ enters the inequality (22) through Eq. (19), and together with $p_{\text{err}}^{(\text{low})}$, they determine the security of the protocol for a given ε . According to Eq. (3), $\langle \hat{Q}_{\tilde{k}}(\theta) \rangle$ and $\langle \hat{Q}_k(\theta) \rangle$ have a common amplitude $\sqrt{2\mu_R}$ given by (3b), and different phases given by Eq. (3c) for k and \tilde{k} , respectively. Throughout this analysis we assume that the adversary aims at emulating the verification of the fixed PUK on a fixed set-up, using his knowledge on the corresponding CRPs [12]. The mean number of scattered photons μ_R that are expected at the verifier's HD set-up, is known to the adversary. Moreover, the adversary knows $\arg(\mathcal{F})$, which is a common fixed phase for both $\langle \hat{Q}_{\tilde{k}}(\theta) \rangle$ and $\langle \hat{Q}_k(\theta) \rangle$, because it depends only on the set-up and the scattering matrix of the PUK which are assumed to be fixed [11]. Thus, $\arg(\mathcal{F})$ is not expected to play any role in the inequality (22), which has been confirmed by our simulations, and the following results and conclusions hold for any value of $\arg(\mathcal{F})$.

Our main findings are presented in Figs. 4 and 5. For all of the combinations of parameters, D exhibits an asymmetric bell-like behavior as a function of N . In particular, there is a critical value of N , say N_c , which depends strongly on μ_R , and weakly on η and on $\bar{\Delta}$. For $N < N_c$, D increases with increasing N , while it decreases for $N > N_c$. This behaviour can be explained by means of Fig. 3, and noting that D is a product of two terms. For small values of N we have $D \simeq 0$, because there is practically no overlap between the possible probe states, and the cheater can discriminate between them (i.e., $p_{\text{err}}^{(\text{low})} \simeq 0$). If we keep increasing N for fixed μ_P , the probe states are coming closer and they start overlap. Hence, $p_{\text{err}}^{(\text{low})}$ becomes non-zero, and increases as we increase N . At the same time, however, the difference of the probabilities on the l.h.s. of (22) decreases, because for any of the quadratures, the photocount distributions associated with neighbouring probes are coming closer. Hence, the origin of an outcome that falls in the expected bin becomes less certain (i.e., the sample may have been obtained from the expected distribution, or from one of its neighbouring distributions). In other words, the server's ability to discriminate between dif-

ferent distributions by looking only at the binned data is gradually lost as we increase N . Given that D is a product of two functions with opposite monotonicity, we have the bell-like behaviour depicted in Figs. 4 and 5.

For typical HD set-ups $\eta \simeq 0.65$, but for the sake of generality we have performed simulations for various values of η , with $0.5 \leq \eta < 1$. Moreover, we consider $4 \leq N \leq 10^3$, which is within reach of the currently available phase modulators (typical precision 0.3-3 mrad). As depicted in Fig. 4(a)-(b), for fixed ε , the range of values of N for which D exceeds 2ε becomes narrower as we decrease η , while the maximum value D_{max} also decreases. However, in practise the detection efficiency is limited by the available technology. Hence, it is sufficient for our purposes to consider the worst-case scenario for the detection efficiency η , which in our case is $\eta = 0.5$. On the contrary, $\bar{\Delta}$ can be chosen as large as possible relative to σ , because it pertains to classical processing of data i.e., the binning of the outcomes from the HDs in M sessions. Following the same reasoning as in the case of η , the optimal value of $\bar{\Delta}$ is the one for which the curve $D(N)$ is as broad and as high as possible. Our simulations suggest that the optimal value is $\bar{\Delta}_{\text{opt}} \simeq 2$ [see Figs. 4(c)-(d)].

Let us consider now the dependence of D on μ_R and N . In view of the findings above, in Fig. 5 we plot D as a function of N and μ_R , for $\eta = 0.5$ and $\bar{\Delta} = 2$, and different values of μ_P . For the reasons explained in Sec. II A, we have focused on $\mu_R \leq 0.7\mu_P$. For a given value of the error ε , each contour refers to combinations of N and μ_R/μ_P for which $D = 2\varepsilon$, and the security condition (22) is satisfied in the enclosed area. For a fixed μ_P , the range of values for N and μ_R for which the security condition is satisfied, becomes broader for decreasing ε (e.g., compare the enclosed areas for different contours in the same plot). The same holds for fixed ε and increasing μ_P (e.g., compare the enclosed areas for the same contour in different plots).

Of course, for practical reasons, one cannot consider arbitrarily small values of ε , because according to (8) the required sample size increases as $\sim \varepsilon^{-2}$. As discussed in Ref. [11], verification tests of error $5 \times 10^{-4} \lesssim \varepsilon \lesssim 1 \times 10^{-3}$ and confidence 99.9% are within reach of today's technology, and ensure security of the protocol in a tamper-resistant scenario. Hence, the contours for 10^{-3} and 2×10^{-3} , are of particular interest, in the sense that they are associated with sample sizes for which the protocol is both practical and cloning-resistant. In both cases, we find that the enclosed (secure) areas are rather broad, which suggests that in practise one has a lot of freedom in choosing N and μ_P , so that the protocol is secure, in spite of the details of the implementation, provided that $\mu_R \gtrsim 0.1\mu_P$.

In closing, it is worth emphasizing that in the absence of related implementations, our simulations have covered a broad range of ratios μ_R/μ_P . In practice, this ratio is expected to be fixed by the verification set-up, and it can be estimated easily by means of related measurements.

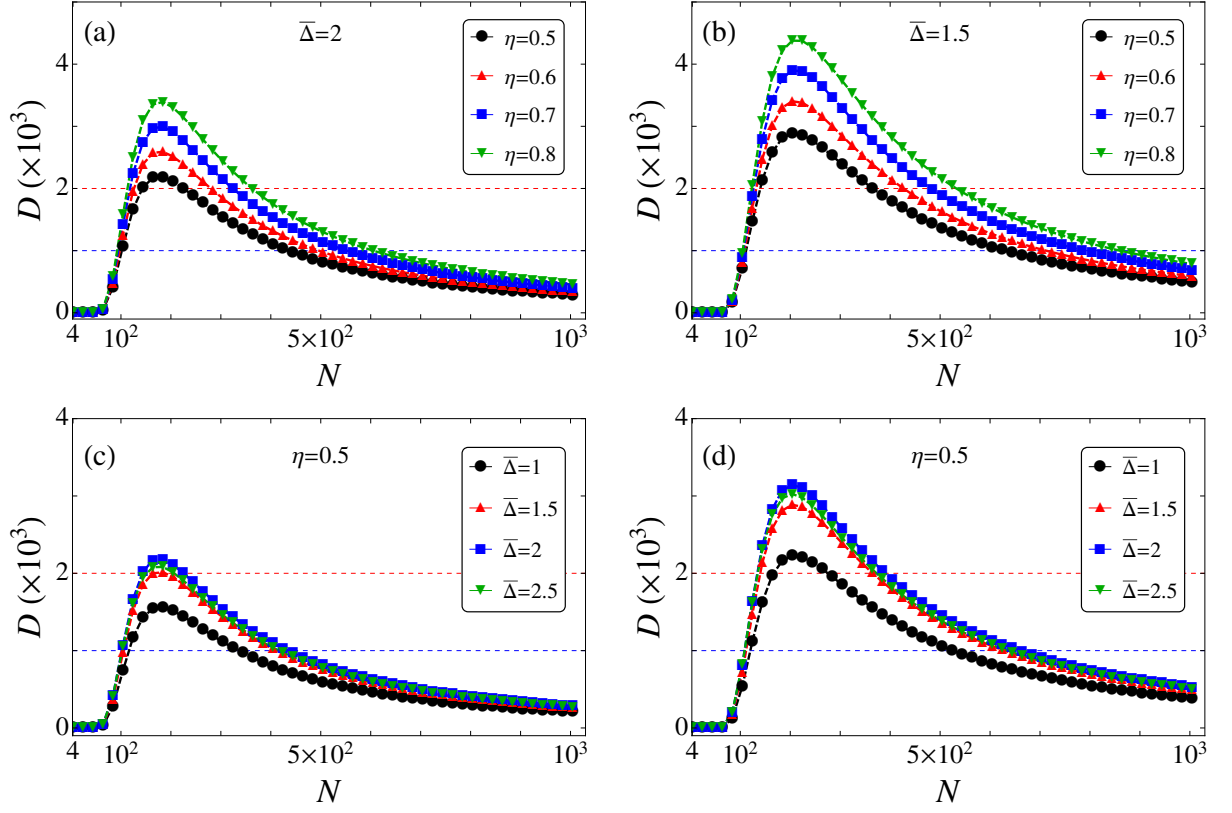


FIG. 4. (Color online) (a,b) The l.h.s of inequality (22) is plotted as a function of the number of phases N , for various values of η and two different values of $\bar{\Delta}$. The horizontal blue and red dashed lines correspond to the right-hand side of (22) for $\varepsilon = 5 \times 10^{-4}$ and $\varepsilon = 10^{-3}$, respectively. The protocol is secure for values N , for which D exceeds 2ε . (c,d) Same as in plots (a,b), but for various values of $\bar{\Delta}$, and fixed $\eta = 0.5$. Other parameters: (a,c) $\mu_P = 600$, $\mu_R = 0.2\mu_P$; (b,d) $\mu_P = 800$, $\mu_R = 0.3\mu_P$.

Hence, using condition (22), one can estimate combinations of μ_P , N and ε , such that the protocol is secure against the emulation attack under consideration.

IV. DISCUSSION

Emulation attack is a very general and powerful attack against EAPs that rely on challenge-response mechanisms, and aims at the impersonation of a legitimate user. Generally speaking, the details of the emulation attack depend strongly on the EAP to be attacked, but the framework is always the same. That is, the verification set-up is not tamper-resistant, and the adversary knows the PIN, and the challenge-response properties of the user's key (conventional chip-based smart card or PUK) [35]. Hence, the adversary's task is to intercept each challenge during the verification stage, read it, and send to the verifier the expected response. Perhaps the most important feature of the emulation attack is that it can be adapted to any EAP, classical or quantum. EAPs that are used for everyday transactions at automatic teller machines, as well as all of the EAPs that rely on

classical read-out of optical [3–8] or electronic PUKs [36], are susceptible to an emulation attack.

In this work we have analysed the security of the EAP of Ref. [11] against an emulation attack, under the assumption of identical enrolment and verification set-ups. The adversary knows the challenge-response properties of the user's PUK and the related PIN, but he does not have access to the laser source, to the detection set-up of the verifier, and to the random choice of the challenges during the verification. Hence, the most likely attack that he can launch is the emulation attack. More precisely, his task is to intercept each quantum challenge during the verification stage, measure it, and send to the verifier's detection set-up the corresponding response. Our analysis is rather general and does not involve any assumptions about the type of the measurement. Using Holevo's bound and Fano's inequality, we derived a sufficient condition for an implementation of the protocol to be secure against the emulation attack. The present results suggest that the protocol of Ref. [11] can be practical, and simultaneously secure against cloning and emulation attack.

For the time being it is not known whether the em-

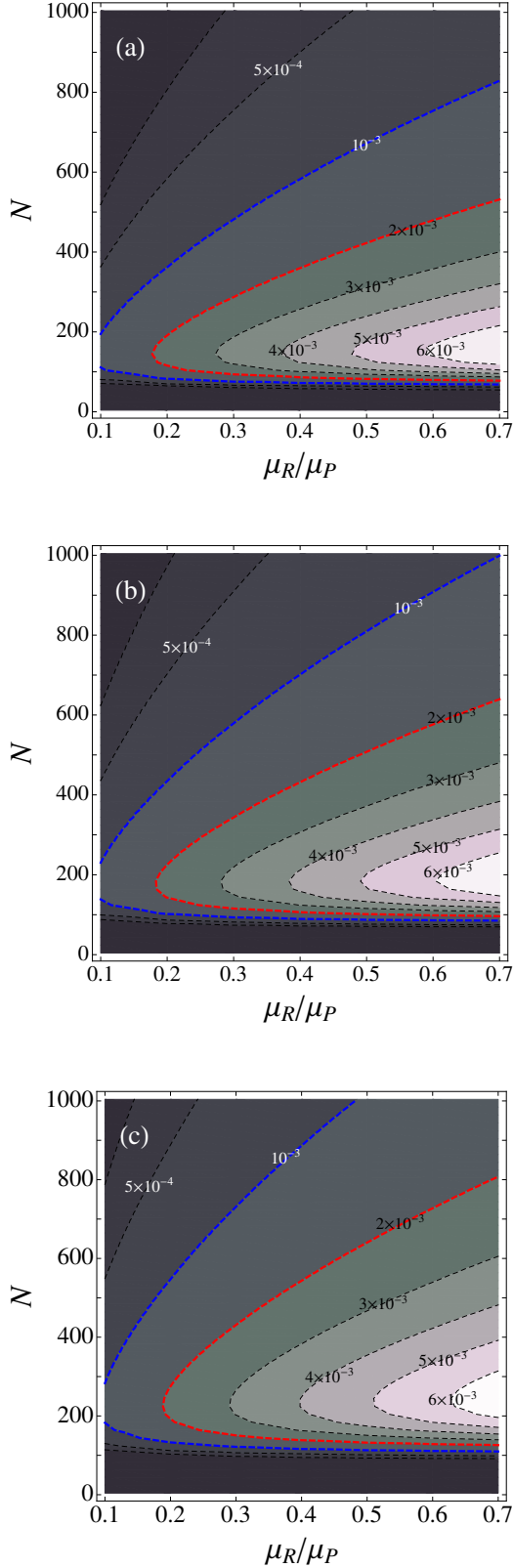


FIG. 5. (Color online) The l.h.s of the security condition (22) is plotted as a function of N and the ratio μ_R/μ_P , for $\mu_P = 400$ (a), 600 (b) and 1000 (c). For given ε , the security condition is satisfied in the area enclosed by the contour $D = 2\varepsilon$. The contours for various values of $\varepsilon \in [1.5 \times 10^{-4}, 3 \times 10^{-3}]$ are shown. Other parameters: $\eta = 0.5$, $\bar{\Delta} = 0.2$.

ulation attack is the most powerful attack against our EAP, under the aforementioned assumptions. As discussed above, the emulation attack is certainly a powerful and general attack, which can break any EAP that relies on classical read-out of optical or electronic PUKs. By contrast, our EAP is robust against the emulation attack, because the PUK is read-out by means of randomly chosen non-orthogonal quantum states.

The security of the present protocol against other types of attacks, in which the adversary has access to various components of the verification set-up (e.g. to the laser source, or the detection device) goes beyond the present theoretical framework, and it is a subject of future theoretical and experimental work. Moreover, the performance of the protocol when the verification set-up deviates from the enrolment set-up (with respect to losses, imperfections, etc), is an interesting question that deserves a thorough investigation (see appendix A). Such deviations are expected to allow for new types of attacks, including perhaps more sophisticated versions of the attack considered in this work.

The emulation attack considered throughout this work can be implemented with today's technology, because it only requires quantum measurements on coherent states of light. An adversary, however, may also attack our EAP using a quantum computer or a large-scale photonic simulator. Related security analysis for the EAP of Ref. [9] suggests that such attacks require simultaneous perfect control of a very large number of quantum states, or optical elements, with negligible losses, which seems to be a formidable challenge for current as well as for future technology. Analogous arguments are expected to be applicable to our scheme as well.

To summarize, quantum-optical EAPs is a very new field of research, with only few relevant publications [9, 11]. There are many open questions about the power and the limitations of such protocols, as well as about the different kinds of attacks and their classification. The present results provide a benchmark case and guide for the planning of future experiments on the protocol of Ref. [11].

Appendix A: Losses

The key component of our EAP is the interrogation chamber, which is a standard wavefront-shaping set-up, and is connected to the laser source and the HD set-up via SMFs A and B, respectively [11]. In the diffusive limit, the operation of the wavefront-shaping set-up can be described in terms of a finite number of transverse spatial modes, say \mathcal{N} input and \mathcal{N} output modes. Adopting an input-output formalism, the mode of SMF A couples to each one of the \mathcal{N} input modes, whereas SMF B is translated at the output plane and couples only to the target mode [11]. The directional transfer of the scattered photons to the target mode is never complete, and part of the input light will be inevitably scattered to the

other output modes. Hence, the amount of control the wavefront shaping offers over the propagation of light is quantified by the enhancement factor \mathcal{E} , which in practise it does not exceed the ideal value of $\pi\mathcal{N}/4$. In addition, to the imperfect concentration of scattered light at the target mode, one expects losses which can be viewed as coupling of the light to other modes, beyond the $2\mathcal{N}$ input/output modes of the wavefront shaping set-up, and the two SMFs.

To account for losses in the interrogation chamber and in the SMFs, we can introduce optical power transmissions τ_{IC} , and $\tau_{A(B)}$, respectively. The mean number of photons at the exit of SMF A is

$$\mu_A = \tau_A \mu_P, \quad (\text{A1})$$

where μ_P is the mean number of photons in the probe state at the entrance of SMF A. The mean number of scattered photons at the entrance of SMF B in the case of optimized SLM is given by [11]

$$\mu_B = \tau_{IC} \mathcal{E} \left[\frac{1}{\mathcal{N}} \left(1 - \frac{l}{L} \right) \right] \mu_A. \quad (\text{A2})$$

In deriving this expression we have assumed slab geometry for the PUK, with thickness L , mean free path l , and absorption length L_{abs} , such that $\lambda \ll l \ll L \ll L_{\text{abs}}$, where λ is the wavelength of the probe. The transmission coefficient $\tau_{IC} \lesssim 1$ accounts for losses in the interrogation chamber, including absorption losses, imperfect couplings etc. The mean number of photons that reach the HD set-up is

$$\mu_R = \tau_B \mu_B. \quad (\text{A3})$$

Combining Eqs. (A1) - (A3) we obtain

$$\mu_R = \mathcal{E} |\mathcal{F}|^2 \mu_P \quad (\text{A4})$$

where

$$|\mathcal{F}|^2 = \tau_B \tau_{IC} \tau_A \left[\frac{1}{\mathcal{N}} \left(1 - \frac{l}{L} \right) \right]. \quad (\text{A5})$$

We see therefore that $|\mathcal{F}|^2$, and thus μ_R , are independent of k , and include all of the losses throughout the propagation of the light in the set-up.

In the security analysis of the present work we assume identical enrolment and verification set-ups. All of the parameters of the set-ups (including losses, imperfections, enhancement, etc), are publicly available (see table II). The mean number of photons that are expected to reach the HD set-up of the verifier, i.e., μ_R , is also publicly known. The security of the EAP relies solely on keeping secret the random, independently chosen phases of the probe states. Acceptance or rejection of the PUK is decided upon the estimated average probability for an outcome to fall in the bin, which is also publicly known.

If the adversary tries to reduce or increase the losses in the set-up, relative to the publicly known values, the verifier will inevitably receive responses that differ from the expected ones both in amplitude (mean number of

photons), and in phase. The security analysis of Sec. III can be adapted to this case as well, by taking into account that $\langle \hat{Q}_k(\theta) \rangle$ will differ from $\langle \hat{Q}_k(\theta) \rangle$, both in phase and in amplitude. In analogy to the discussion of Sec. III, the adversary's intervention will shift the photo-count distributions the verifier samples from, relative to the expected bins. It does not matter whether this shift will be above or below $\langle \hat{Q}_k(\theta) \rangle$, because the r.h.s. of Eq. (14) is an even function of S .

In the envisioned implementation of our EAP, the three major parts of the verification set-up i.e., the laser source, the interrogation chamber and the detection set-up (see Fig. 1), are located in the same or nearby rooms. This means that their separation is tens of meters, and thus the losses in the optical fibers that connect them are negligible. Typically, for optical fibres at 1550 nm, the attenuation coefficient is $\sim 0.2\text{dB/km}$, which means almost perfect transmittance at these distances (i.e., $\tau_{A(B)} \gtrsim 0.99$).

In closing this appendix it is worth pointing out that effects of losses and imperfections may play some role in the security of the protocol, if the verification set-up deviates from the enrolment set-up. This scenario goes beyond the present work, and deserves a careful security analysis, because other types of attacks may be applicable in this case. We strongly believe, however, that for sufficiently small deviations, one can choose the bins' width Δ judiciously so that the protocol tolerates the deviations.

Appendix B: Binning of normal distribution

Consider the normal distribution $\mathcal{N}(\bar{x}, \sigma^2)$, with probability density

$$\mathcal{P}(x) = \frac{1}{\sqrt{2\pi}\sigma^2} \exp\left(-\frac{(x - \bar{x})^2}{2\sigma^2}\right) \quad (\text{B1})$$

and a bin of size Δ centred at $x = b$

$$\left[b - \frac{\Delta}{2}, b + \frac{\Delta}{2} \right].$$

The probability for a random sample from $\mathcal{N}(\bar{x}, \sigma^2)$, to yield an outcome that falls in the bin is given by the following integral

$$\begin{aligned} P_{\text{in}} &= \int_{-\frac{\Delta}{2}}^{\frac{\Delta}{2}} dy \mathcal{P}(y + b) \\ &= \frac{1}{2} \left\{ \text{Erf} \left[\frac{2(\bar{x} - b) + \Delta}{2\sqrt{2}\sigma} \right] - \text{Erf} \left[\frac{2(\bar{x} - b) - \Delta}{2\sqrt{2}\sigma} \right] \right\} \\ &= \frac{1}{2} \left\{ \text{Erf} \left[\frac{2\bar{\xi} + \bar{\Delta}}{2\sqrt{2}} \right] - \text{Erf} \left[\frac{2\bar{\xi} - \bar{\Delta}}{2\sqrt{2}} \right] \right\}, \end{aligned} \quad (\text{B2})$$

where $\text{Erf}(\cdot)$ is the error function, $\xi := \bar{x} - b$, $\bar{\xi} := \xi/\sigma$ and $\bar{\Delta} := \Delta/\sigma$.

We see that P_{in} depends on the distance ξ between the centres of the Gaussian and of the bin, as well as on

the size of the bin Δ , relative to the standard deviation σ . When the centers coincide i.e., for $\xi = 0$, the above expression simplifies to Eq. (5).

Appendix C: Upper bound on probability for in-bin event, in the presence of cheating

Consider a query (sample) with coherent probe state $|\alpha_k\rangle$, which is fully characterized by the randomly chosen integer $k \in \mathbb{Z}_N$. An adversary intercepts and measures the unknown probe state, so that to learn k . Let \tilde{k} denote the adversary's inference, and let $\beta_{\tilde{k}}$ denote the coherent state that is sent to the verifier's HD set-up. The verifier measures at random one of the two quadratures of the electric field, by setting the phase of the LO θ , either to 0, or to $\pi/2$.

The average probability for the verifier to obtain an outcome in the expected bin is given by

$$\begin{aligned} P_{\text{in}} &= \sum_{k, \tilde{k}, \theta} P(\text{in}, k, \tilde{k}, \theta) = \sum_{k, \tilde{k}, \theta} P(\text{in}|k, \tilde{k}, \theta) p(k, \tilde{k}) p(\theta) \\ &= \sum_{k, \theta} P(\text{in}|k, \tilde{k} = k, \theta) p(k, \tilde{k} = k) p(\theta) \\ &\quad + \sum_k \sum_{\tilde{k} \neq k} \sum_{\theta} P(\text{in}|k, \tilde{k}, \theta) p(k, \tilde{k}) p(\theta) \quad (\text{C1}) \\ &:= S_1 + S_2, \end{aligned}$$

where we have used the fact that the angle θ is chosen at random and independently of the choice of k , while the adversary does not have access to the preparation of the probe states, or to the HD set-up. Hence, the inference of the right or wrong value of k by the adversary is independent of the quadrature to be measured by the verifier.

Let us consider first the summation S_1 . The conditional probability $P(\text{in}|k, \tilde{k} = k, \theta)$ is the probability for an outcome to fall in the expected bin, given that the verifier has prepared $|\alpha_k\rangle$, the cheater has inferred the right value of k , and the verifier measures the θ quadrature. Clearly, this probability is given by Eq. (5) (i.e., it is independent of k and θ), because the cheater's intervention has not changed anything relative to the ideal scenario. The joint probability $p(k, \tilde{k} = k)$ is the probability for the verifier to send k , and the cheater to infer

the right value of k . Thus,

$$\sum_k p(k, \tilde{k} = k) = 1 - p_{\text{err}}, \quad (\text{C2})$$

where p_{err} is the average probability for the adversary to infer a wrong value for k . So, we have

$$\begin{aligned} S_1 &= \sum_{k, \theta} P(\text{in}|k, \tilde{k} = k, \theta) p(k, \tilde{k} = k) p(\theta) \\ &= P_{\text{in}}^{(0)} \sum_k p(k, \tilde{k} = k) = (1 - p_{\text{err}}) P_{\text{in}}^{(0)}. \quad (\text{C3}) \end{aligned}$$

We focus now on the second term in Eq. (C1). The joint probability $p(k, \tilde{k})$ is the probability for the verifier to send k , and the cheater to infer a wrong value for k , in the particular case \tilde{k} . Thus, if we sum over all possible values of k and $\tilde{k} \neq k$ we will obtain the average probability of error

$$\sum_k \sum_{\tilde{k} \neq k} p(k, \tilde{k}) = p_{\text{err}}, \quad (\text{C4})$$

which also appears in Fano's inequality (13). So, we have

$$S_2 = \sum_k \sum_{\tilde{k} \neq k} \sum_{\theta} P(\text{in}|k, \tilde{k}, \theta) p(k, \tilde{k}) p(\theta) \quad (\text{C5})$$

$$= \sum_k \sum_{\tilde{k} \neq k} p(k, \tilde{k}) \sum_{\theta=0, \pi/2} P(\text{in}|k, \tilde{k}, \theta) p(\theta) \quad (\text{C6})$$

$$= \sum_k \sum_{\tilde{k} \neq k} p(k, \tilde{k}) P(\text{in}|k, \tilde{k}), \quad (\text{C7})$$

where $P(\text{in}|k, \tilde{k})$ is the conditional probability for an outcome to fall in the expected bin, given that the verifier has prepared $|\alpha_k\rangle$, the cheater has inferred $\tilde{k} \neq k$, irrespective of the measured quadrature.

Hence, using Eq. (C4) we can bound S_2 from above as follows

$$S_2 \leq p_{\text{err}} \max_{k, \tilde{k}} \{P(\text{in}|k, \tilde{k})\}_{\tilde{k} \neq k}. \quad (\text{C8})$$

Using (C3) and (C8) in (C1) we have

$$P_{\text{in}} \leq (1 - p_{\text{err}}) P_{\text{in}}^{(0)} + p_{\text{err}} \max_{k, \tilde{k}} \{\bar{P}(\text{in}|k, \tilde{k})\}_{\tilde{k} \neq k}. \quad (\text{C9})$$

-
- [1] A. Menezes, P. van Oorschot, and Vanstone, S., *Handbook of Applied Cryptography* (CRC Press, Boca Raton, 1996).
 - [2] K. M. Martin, *Everyday Cryptography: Fundamental Principles and Applications* (Oxford University Press, New York, 2012).
 - [3] P. Tuyls, B. Škorić, S. Stallings, A. H. M. Akkermans, and W. Ophey, *Financial Crypto and Data Security* **3**, 141 (2005).
 - [4] R. Horstmeier, S. Assaworrorarit, U. Rührmair, and C. Yang, *IEEE International Symposium on Hardware Ori-*

- ented Security and Trust* (2015).
- [5] R. Pappu, B. Recht, J. Taylor, and N. Gershenfeld, *Science* **297**, 2026 (2002).
- [6] R. Pappu, *Physical One-Way Functions*, Ph.D. dissertation, Massachusetts Institute of Technology (2001).
- [7] J. D. R. Buchanan, R. P. Cowburn, A. Jausovec, D. Petit, P. Seem, G. Xiong, D. Atkinson, K. Fenton, D. A. Allwood, and M. T. Bryan, *Nature* **436**, 475 (2005).
- [8] H. Zhang, and S. Tzortzakakis, *Appl. Phys. Lett.* **108**, 211107 (2016).

- [9] S. A. Goorden, M. Horstmann, A. P. Mosk, B. Škorić, and P. W. H. Pinkse, *Optica* **1**, 421 (2014).
- [10] B. Škorić, A. P. Mosk, and P. W. H. Pinkse, *Int. J. Quant. Inf.* **11**, 1350041 (2013).
- [11] G. M. Nikolopoulos and E. Diamanti, *Sci. Rep.* **7**, 46047 (2017).
- [12] The verification of the PUK takes place only if the server has confirmed the validity of the PIN. If the PIN is not valid, the verification is aborted immediately. Hence, a necessary condition for the emulation attack to take place is the adversary to know the PIN of the user he intends to impersonate, together with the CRPs of the user's PUK. One can assume that the database of CRPs is compromised, and the adversary has obtained a copy of the set of all the CRPs to be used in the verification of the PUK, together with the PIN. Alternatively, one may assume that the adversary has obtained the PIN by other means, and at some point in the past, he has obtained unnoticed access to the PUK for a sufficiently large amount of time, so that to estimate its entire scattering matrix before he returns it to the owner. The security analysis in this work applies to both of these scenarios, although for the sake of concreteness, it is the first one that is mainly mentioned in the text.
- [13] M. A. Nielsen, and I. L. Chuang, *Quantum Computation and Quantum Information* (Cambridge University Press, Cambridge, London, 2000).
- [14] I. M. Vellekoop, and A. P. Mosk, *Opt. Lett.* **32**, 2309 (2007).
- [15] I. M. Vellekoop, and A. P. Mosk, *Opt. Comm.* **281** 3071 (2008).
- [16] A. P. Mosk, A. Lagendijk, G. Lerosey, and M. Fink, *Nature Photon.* **6**, 283 (2012).
- [17] S. R. Huisman, T. J. Huisman, S. A. Goorden, A. P. Mosk, P. W. H. Pinkse, *Opt. Express* **22**, 8320 (2014).
- [18] S. R. Huisman, T. J. Huisman, S. A. Goorden, A. P. Mosk, P. W. H. Pinkse, *Opt. Express* **23**, 3102 (2015).
- [19] S. K. Poppoff, G. Lerosey, R. Carminati, M. Fink, A. C. Boccarda, and S. Gigan, *Phys. Rev. Lett.* **104**, 100601 (2010).
- [20] S. K. Poppoff, G. Lerosey, M. Fink, A. C. Boccarda, and S. Gigan, *New J. Phys.* **13**, 123021 (2011).
- [21] H. Defienne, M. Barbieri, B. Chalopin, B. Chatel, I. A. Walmsley, B. J. Smith, and S. Gigan, *Opt. Lett.* **39**, (2014).
- [22] T. J. Huisman, S. R. Huisman, A. P. Mosk, and P. W. H. Pinkse, *Appl. Phys. B* **116**, 603 (2014).
- [23] T. A. W. Wolterink, R. Uppu, G. Ctistis, W. L. Vos, K. J. Boller, and P. W. H. Pinkse, *Phys. Rev. A* **93**, 053817 (2016).
- [24] H. Yilmaz, W. L. Vos, and A. P. Mosk, *Biomed. Opt. Express* **4**, 1759 (2013).
- [25] B. R. Anderson, R. Gunawidjaja, and H. Eilers, *Phys. Rev. A* **90**, 053826 (2014).
- [26] J. W. Goodman, *Statistical Optics* (John Wiley & Sons, New York, 1985).
- [27] The protocol under consideration can be also implemented with optimized phase mask that changes with the phase of the probe. The analysis of Sec. III A and the security condition (22) are expected to be valid for this case as well, provided one takes into account the dependence of \mathcal{E} and \mathcal{F} on k , when estimating $\max_{k, \tilde{k}} \{P(\text{in}[k, \tilde{k}])\}_{k \neq \tilde{k}}$ in condition (22).
- [28] Here we assume that the server chooses the random challenges and the quadratures to be measured, and sends them to the verifier. Alternatively, one can assume that the verifier obtains a copy of the entire set of CRPs pertinent to the PUK under authentication, and he chooses locally at random and independently the M challenges and the quadratures to be measured. In any case, the verifier should never reveal the sequence of random challenges or the measured quadratures, even after the verification is over.
- [29] We assume that the server has a reliable random number generator (RNG), for the random choice of challenges and quadratures to be measured. Any flaws in the operation of the RNG can be, in principle, exploited by adversaries. Quantum random generators of high quality are currently available on the market [30].
- [30] M. Herrero-Collantes and J. C. Garcia-Escartin, *Rev. Mod. Phys.* **89**, 015004 (2017).
- [31] P. A. Mello, and N. Kumar, *Quantum Transport in mesoscopic system: complexity and statistical fluctuations*, (Oxford University Press, New York, 2004).
- [32] U. Leonhardt, *Essential Quantum Optics: From Quantum Measurements to Black Holes*, (Cambridge University Press, UK, 2010).
- [33] M. G. Raymer, J. Cooper, H. J. Carmichael, M. Beck, and D. T. Smithey, *J. Opt. Soc. Am. B* **12**, 1801 (1995).
- [34] If the verification device is activated only when a PUK is detected to be located in the corresponding slot, then the adversary can insert a false PUK, because he bypasses the interrogation chamber and thus the inserted PUK (true or false), does not play any role in the attack.
- [35] Clearly, if the adversary has stolen the user's PUK, and moreover knows the PIN, he can impersonate successfully the user. In this case, purely cryptographic identification cannot distinguish between the legitimate user and the adversary. To this end, one has to resort to EAPs that rely on biometrics i.e., on physical characteristics of the human body. Such EAPs go beyond the scope of the present work. However, it is worth emphasizing that there are many implementation issues, both technical, practical, and sociological.
- [36] C. Bohm and M. Hofer, *Physical Unclonable Functions in Theory and Practice*, (Springer 2012); M. Roel, *Physically unclonable Functions: Constructions, Properties and Applications*, (Springer 2016).